

Local Energetics Analysis of Blocking Formation in the North Pacific Decomposed in Vertical Mean and Sheared Flows

Yasushi Watarai¹ and H. L. Tanaka²

1: Terrestrial Environment Research Center, University of Tsukuba, Tsukuba, Japan

2: Life and Environmental Science, University of Tsukuba, Tsukuba, Japan, and
Frontier Research Center for Global Change, Japan Agency for Marine-Earth
Science and Technology, Yokohama, Japan

1 INTRODUCTION

Atmospheric blocking is a long-lived and equivalent-barotropic phenomenon with a large amplitude, occurring around the circumpolar region. It causes an abnormal weather owing to its stagnation and persistency. Additionally, it is difficult to predict the blocking state, especially near the onset time.

Tanaka and Kung (1988) performed the three-dimensional global energetics, and found the energy transformation from the synoptic-scale baroclinic to the planetary-scale barotropic component, prior to the onset of blocking. It suggests the importance of the contribution from the barotropic-baroclinic interactions during the formation of blocking.

Watarai and Tanaka (2002) investigated the characteristics of the barotropic-baroclinic interactions in the kinetic energy equations divided in the vertical mean and sheared flows. They showed that the barotropic-baroclinic interactions were intensified in both the western and eastern flanks of the blocking ridge, by the composite of 10 blocking events. However, a further analysis is required in order to identify the condition of the blocking formation.

The objective of this study is to investigate the condition of the blocking formation based on a comprehensive energetics, using a number of samples. First, we examine the sensitivity of the ridge for the intensity of barotropic-baroclinic interactions. We then compare the blocking and the non-blocking from the viewpoint of the local kinetic energetics.

2 EQUATIONS AND DATA

In this study, the kinetic energy equations were divided in the vertical mean (barotropic) and sheared (baroclinic) components. The barotropic and baroclinic components for a field variable, ξ , are defined the following:

$$\xi_m = \frac{1}{p_s} \int_0^{p_s} \xi dp, \quad \xi_s = \xi - \xi_m, \quad (1)$$

where p_s is the surface pressure. Hereafter, the barotropic and baroclinic components are designated by the subscripts m and s , respectively.

By making use of (1), the equation of vertical-integrated kinetic energy (K) can be written as follows (see Watarai and Tanaka 2004):

$$\frac{\partial K_m}{\partial t} = B(K_m + \Phi_m) + C(K_s, K_m) - D(K_m), \quad (2)$$

$$\frac{\partial K_s}{\partial t} = B(K_s + \Phi_s) + C(A, K_s) - C(K_s, K_m) - D(K_s), \quad (3)$$

where Φ is the geopotential, and A the vertical-integrated available potential energy. The term $B(K_m + \Phi_m)$ is the flux convergence of mechanical energy (i.e., the sum of kinetic and potential energy), and $D(K_m)$ the dissipation of kinetic energy, in the barotropic flow. The term $C(K_s, K_m)$ is the conversion of kinetic energy from the baroclinic to the barotropic component, and $C(A, K_s)$ the conversion from available potential energy to baroclinic kinetic

energy. Since the blocking anticyclone is characterized by the equivalent-barotropic structure, we assumed that the blocking formation was understood by the budget of barotropic kinetic energy. Equation (2) was used in order to examine the blocking formation in this study.

The data in this study were the NCEP/NCAR reanalysis for 51 winter seasons (November to March) from 1950/51 to 2000/01, with the time interval of six hours (Kalnay et al. 1996). The grid resolution of the data is 2.5° by 2.5° of zonal/meridional directions, and 17 pressure levels of vertical direction.

3 INDICES

In order to identify a lot of events objectively, a “B-index”, defined by Lejenäs and Økland (1983), was used. This is defined as the local difference in 500-hPa geopotential height at 40°N , subtracted from that at 60°N . When the index was negative, as seen for a high-pressure mass staying around 60°N , the situation was considered as a low-index event. In this study, only the low-index events occurred in the North Pacific sector (ranged from 140°E to 130°W) were picked up. The total of 452 low-index events were extracted during 51 winters.

However, a low-index event is not always regarded as a blocking, because each of event has a variety of duration and the persistency is one of the characteristics of blocking. For example, the number of low-index events lasting at least 7 days was 88 during the 51 winters. On the other hand, 253 of the low-index events lasted less than 3 days.

According to Watarai and Tanaka (2002), a positive $C(K_s, K_m)$ around the ridge plays an important role in forming a blocking anticyclone. In order to represent the intensity of $C(K_s, K_m)$ around a blocking, another index (named “C-index”) was introduced. For each of the low-index events, we first evaluated the average of $C(K_s, K_m)$ over -30° to $+30^\circ$ in longitude, and 50°N to 70°N in latitude, from the center of the B-index minimum. The C-index was then defined by the time average of it between -3 and $+3$ days from the onset of the low-index event.

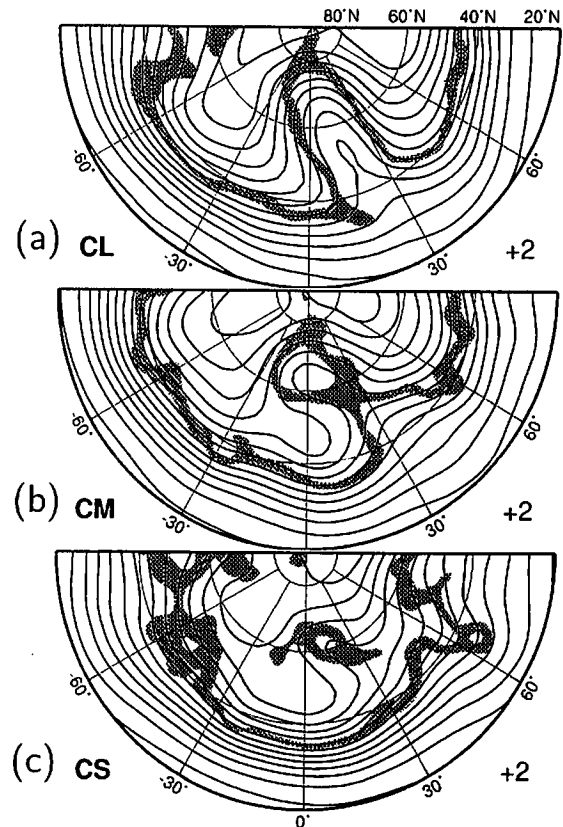


Figure 1: Composite maps of geopotential height (solid lines) and the approximated isobaric PV (Nakamura and Wallace 1993) ranged from 3 to 4 PVU (shading) at 250-hPa level at +2 days relative to the onset time for (a) CL, (b) CM and (c) CS. The longitude is represented by the relative one from the center of the B-index minimum. Contour interval is 100 m.

Four groups were selected from the low-index events in this study. First, we picked up 10 events with the largest C-index from 88 long-lived (≥ 7 days) events, and a group of them was labeled “CL”. In order to examine the sensitivity of the C-index for the long-lived events, 10 events with the smallest and the medium C-index are then chosen, and named “CS” and “CM”, respectively. On the other hand, 21 events with the C-index more than the lower limit of CL (5.02 Wm^{-2}) were also picked up from the short-lived (< 3 days) events.

4 RESULTS

Figure 1 illustrates the composite maps of geopotential height and potential vorticity (PV) at 250-hPa level, at +2 days from the onset time of events.

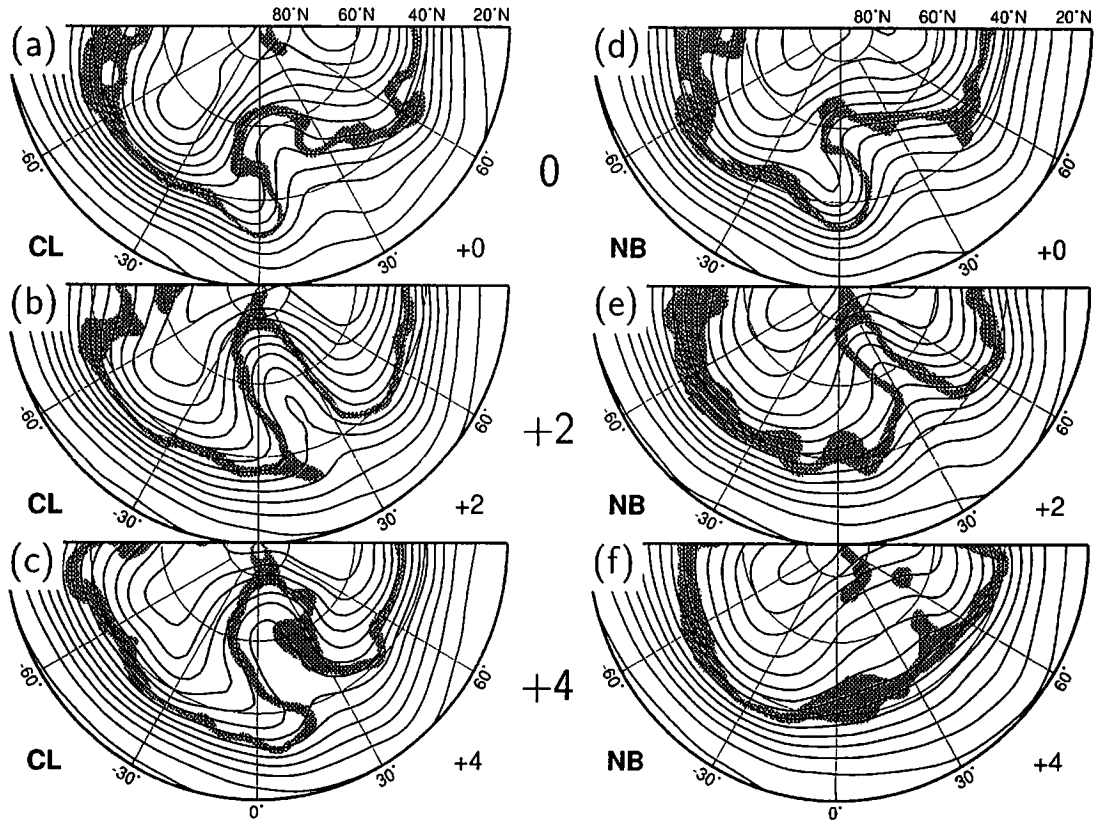


Figure 2: CL (left; a-c) and NB (right; d-f) composite maps of geopotential height and isobaric PV at 250-hPa level, as in Fig. 1. Maps at 0 (top), +2 and +4 (bottom) day(s) from the onset time are displayed.

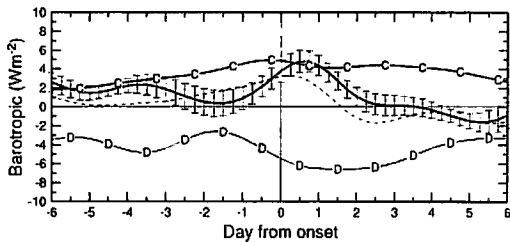
In the CL composite, low-PV air thrusts into poleward air deeply, and a pronounced blocking of the Ω type with strong polar jet is formed (Fig. 1a). In the CM composite, the meridional gradient of PV overturns, and there appear a double-jet pattern, around the center (Fig. 1b). The strength of poleward jet in CM is weaker than in CL, and the spatial pattern shows a dipole-type blocking. In contrast, cut-off low-PV is very weak and composite pattern is no longer a blocking in CS events whose C-indices are almost zero (i.e., averaged index of 0.21 Wm^{-2}).

Figure 2 illustrates the composite maps of (a-c) the CL and (d-f) the NB events at 0, +2 and +4 days from the onset time. As is mentioned above, the ridge grows in meridional direction and becomes the Ω -type blocking in the CL events. Formed blocking maintains its intensity and is almost stationary. As for the NB composite, 250-hPa geopotential height and PV fields are similar to the CL, and the inversion of meridional PV gradient occurs around the

centered longitude, at the onset time. Although the low-PV air intrudes deeply into high latitudes, the ridge moves eastward and become narrower. At last, the ridge is attenuated, and the flow about $+30^\circ$ from the centered longitude becomes more zonal.

Figure 3 shows the time series of the terms in Eq. (2) averaged in the ridge area for (a) the CL and (b) the NB composites. In both composites, positive K_m tendency (dashed line) gradually increases and reaches about 3 Wm^{-2} at the onset time. Thereafter, K_m tendency decreases in both composites, but the NB decreases more rapidly than the CL. These two composites are similar in the time series of $C(K_s, K_m)$, since the selected events have large values of C-index in both composites. However, the time series of $B(K_m + \Phi_m)$ (thick solid line) is different between the CL and the NB. In the CL composite, $B(K_m + \Phi_m)$ is roughly zero or positive. It is comparable to $C(K_s, K_m)$ at the onset time, and becomes about zero after day +2. In the NB com-

(a) CL



(b) NB

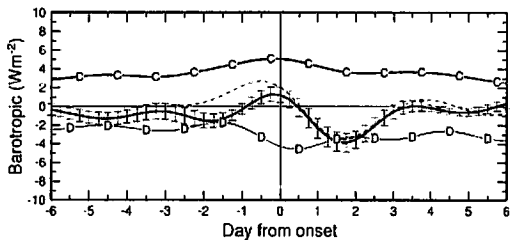


Figure 3: Time series of the K_m tendency (dashed line), $B(K_m + \Phi_m)$ (thick solid line), $C(K_s, K_m)$ (labeled “C”) and the residual dissipation term, $D(K_m)$ (labeled “D”) for (a) CL and (b) NB composites. All values are averaged in the ridge area ranged from -30° to 45° in longitude, and from 50°N to 80°N in latitude. As for $B(K_m + \Phi_m)$, the bars of standard error are also represented.

posite, on the other hand, it is less than half of $C(K_s, K_m)$ at the onset. At day +2, it reaches the minimum value (about -4 Wm^{-2}), which is comparable to $C(K_s, K_m)$, but the opposite sign.

5 CONCLUSION

In this study, local energetics analysis is performed in the North Pacific to find the condition of the blocking formation. The total of 452 low-index events are extracted during the 51 winters from 1950/51 to 2000/01, using the index of Lejenäs and Økland (1983). Among them, 88 and 253 events lasted more than 7 and less than 3 days, respectively. The C-index is defined to measure the intensity of the barotropic-baroclinic interactions.

We first examined the sensitivity of the C-index for the long-lived events. As a result, it is found that a blocking becomes an Ω type for the CL events having large $C(K_s, K_m)$. It is consistent with the results of Watarai and Tanaka (2002). In addition, a blocking becomes a dipole type for medium C-index (CM). If

$C(K_s, K_m)$ around the ridge is almost zero (i.e., CS), the ridge is, however, no longer a blocking. Therefore, it is suggested that the positive $C(K_s, K_m)$ is a necessary condition for the blocking formation.

However, there are some non-blocking events with a large C-index. As a result of the comprehensive kinetic energy budget, specific difference between the blocking (CL) and the non-blocking (NB) is found; a positive contribution of $B(K_m + \Phi_m)$ around the ridge in CL and a negative in NB. Therefore, it is suggested that the positive value of the flux convergence of mechanical energy around the transient ridge is another necessary condition for the ridge to become a blocking.

References

- Kalnay, E., M. Kanamitsu, R. Kistler, W. Collins, D. Deaven, L. Gandin, M. Iredell, S. Saha, G. White, J. Woollen, Y. Zhu, M. Chelliah, W. Ebisuzaki, W. Higgins, J. Janowiak, K. C. Mo, C. Ropelewski, J. Wang, A. Leetmaa, R. Reynolds, R. Jenne and D. Joseph, 1996: The NCEP/NCAR 40-year reanalysis project. *Bull. Amer. Meteor. Soc.*, **77**, 437–471.
- Lejenäs, H. and H. Økland, 1983: Characteristics of Northern Hemisphere blocking as determined from a long time series of observational data. *Tellus*, **35A**, 350–362.
- Nakamura, H. and J. M. Wallace, 1993: Synoptic behavior of baroclinic eddies during the blocking onset. *Mon. Wea. Rev.*, **121**, 1892–1903.
- Tanaka, H. L. and E. C. Kung, 1988: Normal mode energetics of the general circulation during the FGGE year. *J. Atmos. Sci.*, **45**, 3723–3736.
- Watarai, Y. and H. L. Tanaka, 2002: Characteristics of barotropic-baroclinic interactions during the formulation of blocking events in the Pacific region. *J. Meteor. Soc. Japan*, **80**, 387–402.
- Watarai, Y. and H. L. Tanaka, 2004: Local energetics analysis of blocking formation in the North Pacific decomposed in vertical mean and sheared flows. *J. Meteor. Soc. Japan*, **82**, (accepted).